

High-energy emission from pulsars in polar-cap models with CR-induced cascades

B. Rudak & J. Dyks

N. Copernicus Astronomical Center, Rabiańska 8, 87-100 Toruń, Poland

e-mail: bronek@camk.edu.pl, jinx@astri.uni.torun.pl

Accepted 1998 November 30. Received 1998 June 2; in original form 1997 March 4

ABSTRACT

For a subclass of polar-cap models based on electromagnetic cascades induced by curvature radiation (CR) we calculate broad-band high-energy spectra of pulsed emission expected for classical and millisecond pulsars. The spectra are a combination of curvature and synchrotron components. The spectrum of curvature component breaks at 150 MeV, and neither its slope nor level below this energy are compatible with phase-averaged spectra of pulsed X-ray emission inferred from observations. Spectral properties in the combined energy range of *ROSAT* and *ASCA* (0.1 - 10 keV) depend upon the location of cyclotron turnover energy $\epsilon_{ct} = \hbar \frac{eB}{m_e c} / \sin \psi$ in the synchrotron component. Unlike in outer-gap models, the available range of pitch angles ψ is rather narrow and confined to low values. For classical pulsars, a gradual turnover begins already at ~ 1 MeV, and the level of the synchrotron spectrum decreases. At ~ 10 keV the curvature component eventually takes over, but with photon index $\alpha = 2/3$, in disagreement with observations.

For millisecond pulsars, the X-ray spectra are dominated by synchrotron component with $\alpha \simeq 1.5$, and a sharp turnover into $\alpha \simeq -1$ at $\epsilon_{ct} \sim 100$ eV.

Relations of pulsed luminosity L_X to spin-down luminosity L_{sd} are presented for classical and millisecond pulsars. We conclude that spectral properties and fluxes of pulsed non-thermal X-ray emission of some objects, like the Crab or the millisecond pulsar B1821-24, pose a challenge to the subclass of polar-cap models based on curvature and synchrotron radiation alone.

Key words: pulsars: general - X-rays: observations - X-rays: theory

1 INTRODUCTION

According to recent results from *ROSAT* and *ASCA* (Becker & Trümper 1997 and Saito 1998, respectively) luminosities of pulsed and unpulsed components in the X-ray emission from pulsars are related to spin-down luminosities L_{sd} , suggesting thus a rotation-powered origin of X-rays. The unpulsed emission is usually interpreted as synchrotron radiation from an unresolved nebula surrounding the pulsar. A magnetospheric wind of ultrarelativistic particles (with Lorentz factors about 10^7) will lead to X-ray emission provided the nebula contains magnetic field of the order of $\sim 10^{-4}$ G (e.g. Manning & Willmore (1994) estimate the magnetic field strength of 0.17×10^{-4} G for the hypothetical nebula around B0950+08).

Pulsed components are of particular interest, since they are the direct signatures of non-thermal processes within a magnetosphere. Very likely, pulsed non-thermal X-ray emission is nothing but a low-energy tail of gamma-ray emission,

which in most models is a superposition of curvature (CR) and synchrotron (SR) emission. In a subclass of polar cap models developed by Dermer & Sturmer (1994) gamma-ray photons have different origin - they are thermal UV/X-ray photons subject to Lorentz-boost by inverse Compton scattering (IC) with beam particles.

In polar-cap scenarios pulses in gamma-rays should be accompanied by pulses in X-rays, with similar shapes, and in phase. With such criteria the Crab pulsar would be a model example. However, one has to show first that its contributions to X-rays and gamma-rays are in right proportions, i.e. in (at least qualitative) accord with model predictions.

Phase-averaged broad-band ($X\gamma$) spectra of six, out of seven, gamma-ray pulsars are relatively steep, with photon index $\alpha_{X\gamma}$ decreasing with pulsar's characteristic age (see Thompson et al. 1997 for recent review):

For the Crab $\alpha_{X\gamma} \approx 2$, and therefore, luminosities per logarithmic energy bandwidth in X-rays and in gamma-rays are comparable. For B1055-52, which is the oldest gamma-ray

pulsar, $\alpha_{X\gamma} \approx 1.6$, and its pulsed X-ray luminosity L_X is roughly one per cent of its L_γ .

[Note: To make this comparison we followed the convention used in gamma-rays ($\Omega_\gamma = 1$ sr is the solid angle of gamma-ray emission) taking $\Omega_X = 1$ sr for the solid angle of X-ray emission.]

These observed spectral properties have been quite successfully accounted for in a newly proposed model of ‘thick outer gap’ by Zhang & Cheng (1997). Unlike polar-cap models, outer-gap models [see also Wang et al. (1997)] may take advantage of the full range of pitch angles, which in turn makes it possible to trigger electromagnetic cascades even for relatively soft gamma-ray photons ($\gtrsim 1$ MeV) on magnetic field lines (also on closed ones). The energy distribution function for e^\pm pairs produced in the cascades may easily become steep enough ($N(\gamma_\pm) \propto \gamma_\pm^{-3}$) over a wide range of energy, for subsequent synchrotron spectrum ($\alpha_{X\gamma} = 2$) to account for the observed soft gamma-rays and X-rays. In particular, Cheng et al. (1998) managed to reconstruct simple empirical relation between L_X and L_{sd} , which reads (assuming $\Omega_X = 4\pi$ sr) $L_X \simeq 10^{-3} L_{sd}$ (Becker & Trümper 1997). Moreover, cascades propagating starward are subject to substantial lateral spread, leading thus to rather weak X-ray modulations.

The aim of this paper is to present general features of broad-band $X\gamma$ spectra expected for the subclass of polar cap models, with $X\gamma$ emission due to CR and SR (e.g. Daugherty & Harding 1982, Daugherty & Harding 1996) and to show that luminosity of pulsed X-rays observed for some pulsars is too high compared to L_γ (or to L_{sd} if there is no information about gamma-rays) to be understood within polar-cap models unless some unorthodox assumptions are accepted. Some of these features are only weakly model-dependent and may, therefore, play a decisive role in assessing validity of polar-cap models. We were motivated by the fact, that neither proponents nor oponents of the polar-cap models seem to acknowledge a real challenge posed to these models by observed properties of non-thermal, pulsed X-ray emission. It is this emission which is more promising as a potential discriminator between rivaling classes (polar-cap, outer-gap) of models than gamma-ray emission itself. In Section 2 we present model spectra of CR and SR emission per parent (beam) particle, expected in pulsars with high ($\sim 10^{12}$ G) and low ($\sim 10^9$ G) magnetic fields. Section 3 compares L_X expected within energy band 0.1 keV – 10 keV with observations for a wide range of spin-down luminosities L_{sd} . Section 4 contains discussion and conclusions.

2 SPECTRAL PROPERTIES OF CURVATURE AND SYNCHROTRON RADIATION

The energy distribution $N_e(\gamma)$ of particles is governed by their injection rate $Q_e(\gamma)$ (also called a source function), cooling rate $\dot{\gamma}$, and a characteristic time scale of their escape t_{esc} , via steady-state kinetic equation

$$\frac{\partial}{\partial \gamma}(|\dot{\gamma}|N_e) = N_e/t_{esc} - Q_e, \quad (1)$$

where γ is particle energy in units of $m_e c^2$.

The solution of eq.1 yields two asymptotic relations

$$N_e(\gamma) = \begin{cases} \frac{1}{|\dot{\gamma}|} \int_\gamma^{\gamma_{\max}} Q_e(\gamma) d\gamma, & |\dot{\gamma}|/\gamma \gg t_{esc}^{-1}; \\ Q_e \cdot t_{esc}, & |\dot{\gamma}|/\gamma \ll t_{esc}^{-1}. \end{cases} \quad (2)$$

If the solution to eq.1 is a power-law function with index p , $N_e \propto \gamma^{-p}$, the subsequent photon spectrum of SR or CR will have a form

$$N_\nu(\epsilon) \propto \epsilon^{-\frac{p+1}{q}}, \quad (3)$$

(but the value of p must not be too low) where $q = 2$ for SR, or $q = 3$ for CR.

[Note: Throughout this section we use a short notation for electron and photon distribution functions: $N_e(\gamma) = dN_e/d\gamma$ and $N_\nu(\epsilon) = dN_\nu/d\epsilon$, respectively.]

2.1 Curvature Radiation

First, let us consider spectral component due to CR. If the source function $Q_e(\gamma)$ of beam particles is monoenergetic

$$Q_e(\gamma) = C_0 \delta(\gamma_0 - \gamma), \quad (4)$$

and redistribution over the energy space is governed by the CR cooling ($|\dot{\gamma}| = |\dot{\gamma}_{cr}| \propto \gamma^4$), then from the first relation of eq.2 it follows that $N_e \propto \gamma^{-4}$ (i.e. $p = 4$) for $\gamma < \gamma_0$. The lower limit (let us denote it as γ_{break}) to this distribution is determined by the condition, that a cooling time-scale due to CR, $t_{cr} \equiv \gamma/|\dot{\gamma}_{cr}|$, is shorter than t_{esc} . According to eq.3, the photon spectrum of CR becomes $N_{cr}(\epsilon) \propto \epsilon^{-\frac{5}{3}}$. It remains unchanged down to photon energy ϵ_{break} , which may be approximated with a characteristic energy of CR

$$\epsilon_{crit} = \frac{3}{2} c \hbar \frac{\gamma^3}{\rho_{cr}}, \quad (5)$$

(where ρ_{cr} is a local radius of curvature) taken for γ_{break} . Below ϵ_{break} , the photon spectrum follows the low-energy tail of CR, i.e. $N_{cr}(\epsilon) \propto \epsilon^{-\frac{2}{3}}$. In order to find ϵ_{break} we should first estimate the time scale t_{esc} . We assume that $t_{esc} \approx \rho_{cr}/c$. The CR cooling rate for a single particle of energy γ is

$$\dot{\gamma}_{cr} = -\frac{2}{3} \frac{e^2}{mc} \frac{\gamma^4}{\rho_{cr}^2}. \quad (6)$$

The condition $t_{cr} = t_{esc}$ becomes then

$$\frac{\gamma_{break}^3}{\rho_{cr}} = \frac{3}{2} \frac{mc^2}{e^2}, \quad (7)$$

and from eq.5 it follows that

$$\epsilon_{break} = \frac{9}{4} \hbar \frac{c}{r_0} \approx 150 \text{ MeV}, \quad (8)$$

where r_0 is the classical electron radius. Note, that the photon energy ϵ_{break} at which the spectral break occurs does not depend on any pulsar parameters, as long as our estimation of t_{esc} is accurate. In particular, it does not depend on magnetic field structure - should it be pure dipole with $\rho_{cr} \gtrsim 10^8 \sqrt{P}$ cm, or dominated by high-order multipolar components with $\rho_{cr} \sim 10^6$ cm.

Fig.1 shows numerically calculated shapes of the CR spectrum produced by beam particles injected at the outer rim of a canonical polar cap with a dipolar magnetic field. The magnetic strength B_{pc} at the polar cap is 10^9 G (upper panel), and 10^{12} G (lower panel). The period of rotation P is 0.003 s and 0.06 s, respectively. For the initial energy E_0

we choose 1.1×10^7 MeV and 6.7×10^6 MeV, respectively (see section 3 for explanation). The dotted line corresponds to the unabsorbed spectrum, and the solid line is the spectrum with magnetic absorption. The spectral break (where the power-law spectrum changes its slope by one power of ϵ) is visible in both panels, and its location at ~ 150 MeV agrees quite well with the analytical estimate (eq.8). A word of comment on high-energy cutoffs seems appropriate here, though it is not linked directly to the subject of this paper: The high-energy cutoff for the case of 10^{12} G does not exceed 10 GeV, whereas the cutoff for the low- B case reaches ~ 0.1 TeV (the energy range accessible with ground-based Cherenkov techniques). The explanation is twofold: (1) for low values of B the magnetic absorption is weak; (2) very short periods P infer small dipolar curvature radii, and a characteristic photon energy (eq.5) taken for $\gamma_0 = E_0/m_e c^2$ increases.

With the spectral break at $\epsilon_{\text{break}} \approx 150$ MeV, the curvature radiation becomes energetically unimportant below this energy. Such objects would be dim in X-rays, which apparently is not the case. Moreover, the slope $-2/3$ in the X-ray energy range is in clear conflict with spectral analysis of X-ray data (Becker & Trümper 1997).

A way out may be offered by including synchrotron radiation (next subsection) and/or by relaxing the assumption about the monoenergetic source function of beam particles (eq.4). Suppose, for example, that we want the slope of $-5/3$ to extend down to energy ϵ_x in the X-ray range: $N_\nu(\epsilon) \propto \epsilon^{-5/3}$ for $\epsilon \gtrsim \epsilon_x$. According to eq.2 (lower relation) we now have the energy distribution $N_e(\gamma) = Q_e \cdot t_{\text{esc}}$. This, in turn, requires that the source function of beam particles is

$$Q_e \propto \gamma^{-4}, \text{ for } \gamma \gtrsim \gamma_x, \quad (9)$$

a very steep function of γ (for whatever the reason), where γ_x is linked to ϵ_x via eq.5. To find γ_x we solve the equation $\epsilon_x = \epsilon_{\text{crit}}(\gamma_x)$ for γ_x : For dipolar magnetic fields, the smallest curvature radii ρ_{cr} are those at outer rim of the polar cap. They may be approximated with $\rho_{\text{cr}} \approx \sqrt{r R_L}$, where r is the radial coordinate of the particle, and $R_L = cP/2\pi$ is the pulsar's light cylinder. Within the region of $r \simeq 2R_{\text{NS}}$ we have therefore $t_{\text{esc}} \approx 10^{-2.5} \sqrt{P}$ s. From eq.5 we obtain

$$\epsilon_x \approx 0.3 (\gamma_x/10^5)^3 P^{-0.5} \text{ keV}. \quad (10)$$

For a pulsar with $P = 0.1$ s, the source function $Q_e(\gamma) \propto \gamma^{-4}$ would have to extend down to $\gamma_x \sim 10^5$ for ϵ_x to reach ~ 1 keV. This value of γ_x is about 55 times lower than the value of γ_{break} (eq.7) corresponding to ϵ_{break} (eq.8).

2.2 Synchrotron Radiation

Since CR is not a promising candidate for hard X-rays, the standard explanation involves SR, produced by e^\pm pairs created in the process of magnetic absorption of high-energy CR photons. Total contribution of the SR component to the overall (SR+CR) energy of radiation per beam particle depends on number of created pairs n_\pm . One may expect, therefore, that at least for pulsars with strong magnetic fields ($\sim 10^{12}$ G), the energy contained in SR should be comparable or exceed the energy contained in CR. However, spectral properties of the SR component depend not only on local values of B , but also on the available range of

pitch angles ψ between magnetic field lines and the direction of propagation of created pairs. The most popular assumption – about an isotropic distribution – may be fully justified in the case of outer-gap models (Zhang & Cheng 1997), but is not obvious by any means for polar-cap scenarios.

Below, we'll present numerical calculations of synchrotron spectra due to e^\pm -pairs which are assumed (after Daugherty & Harding 1982) to be directed along the direction of propagation of their parent CR-photons at the moment of the creation. This assumption, along with narrow opening angles of magnetic field lines available for beam particles, results in a confinement of pitch angles to a narrow range of low values. For a pulsar with a dipolar magnetic field and rotating with period P , we expect then $\sin \psi \leq 0.01/\sqrt{P}$ as a first approximation.

The character of the source function Q_\pm of e^\pm -pairs depends primarily on the reachness of the cascades. In the case of low magnetic fields ($\sim 10^9$ G) only one generation of e^\pm -pairs is produced, and their formation region is narrow. For these reasons Q_\pm is almost monoenergetic (see Fig.1, upper panel), and basic spectral properties of SR calculated for a canonical millisecond pulsar are easily understood with well known analytical considerations:

Let us denote by γ_\parallel the particle Lorentz factor along the local magnetic field line. We will ignore possible curvature of the line, and assume that γ_\parallel remains constant. The particle energy (in units of $m_e c^2$) to be emitted in bursts of SR corresponds then to Lorentz factor γ_\perp of gyration. The total particle energy is $\gamma = \gamma_\perp \gamma_\parallel$. As long as $\gamma_\parallel \gg 1$, the pitch angle of the particle is determined by $\sin \psi \approx \gamma_\parallel^{-1}$.

The rate of SR cooling is

$$\dot{\gamma}_{\text{sr}} = -\frac{2}{3} \frac{r_0^2}{m_e c} B^2 \gamma_\perp^2 = -\frac{2}{3} \frac{r_0^2}{m_e c} B^2 \sin^2 \psi \gamma^2. \quad (11)$$

Unlike in the case of CR, the SR cooling rate is enormous and affects the energy distribution of pairs until $\gamma_\perp \sim 1$ where the synchrotron approximation breaks (O'Dell & Sartori 1970). Therefore, from eqs.2, 11 and 3, we'll get photon spectrum of SR with well known single power-law shape $N_{\text{sr}}(\epsilon) \propto \epsilon^{-3/2}$. Main contribution to the spectrum at energy ϵ comes from particles with γ for which $\epsilon = \epsilon_{\text{sr}}(\gamma)$, where

$$\epsilon_{\text{sr}} = \frac{3}{2} c \hbar \frac{eB}{m_e c} \gamma^2 \sin \psi, \quad (12)$$

is a critical photon energy in SR. The spectrum spreads between a high-energy cutoff $\epsilon_{\text{sr}}(\gamma_{\text{max}})$ and a low-energy turnover ϵ_{ct} determined by the condition $\gamma_\perp \sim 1$ (O'Dell & Sartori 1970):

$$\epsilon_{\text{ct}} \equiv \epsilon_{\text{sr}}(\gamma = \gamma_\parallel) = \frac{3}{2} c \hbar \frac{eB}{m_e c} \frac{1}{\sin \psi}. \quad (13)$$

Below ϵ_{ct} , the spectrum flattens, and may be described asymptotically as $N_{\text{sr}}(\epsilon) \propto \epsilon^{+1}$. It is built up by contributions from low-energy tails emitted by particles with $\gamma_\perp \gg 1$, and each low-energy tail is assumed to cut off at local gyrofrequency, which in the reference frame comoving with the center of gyration is $\omega_B = \frac{eB}{m_e c \gamma_\perp}$.

The numerical example presented in the upper panel of Fig.1 reveals all these 'classical textbook' features so clearly, because (for reasons mentioned before) the source function of pairs in the case of a dipolar field with $B_{\text{pc}} = 10^9$ G is practically monoenergetic. The turnover energy is located

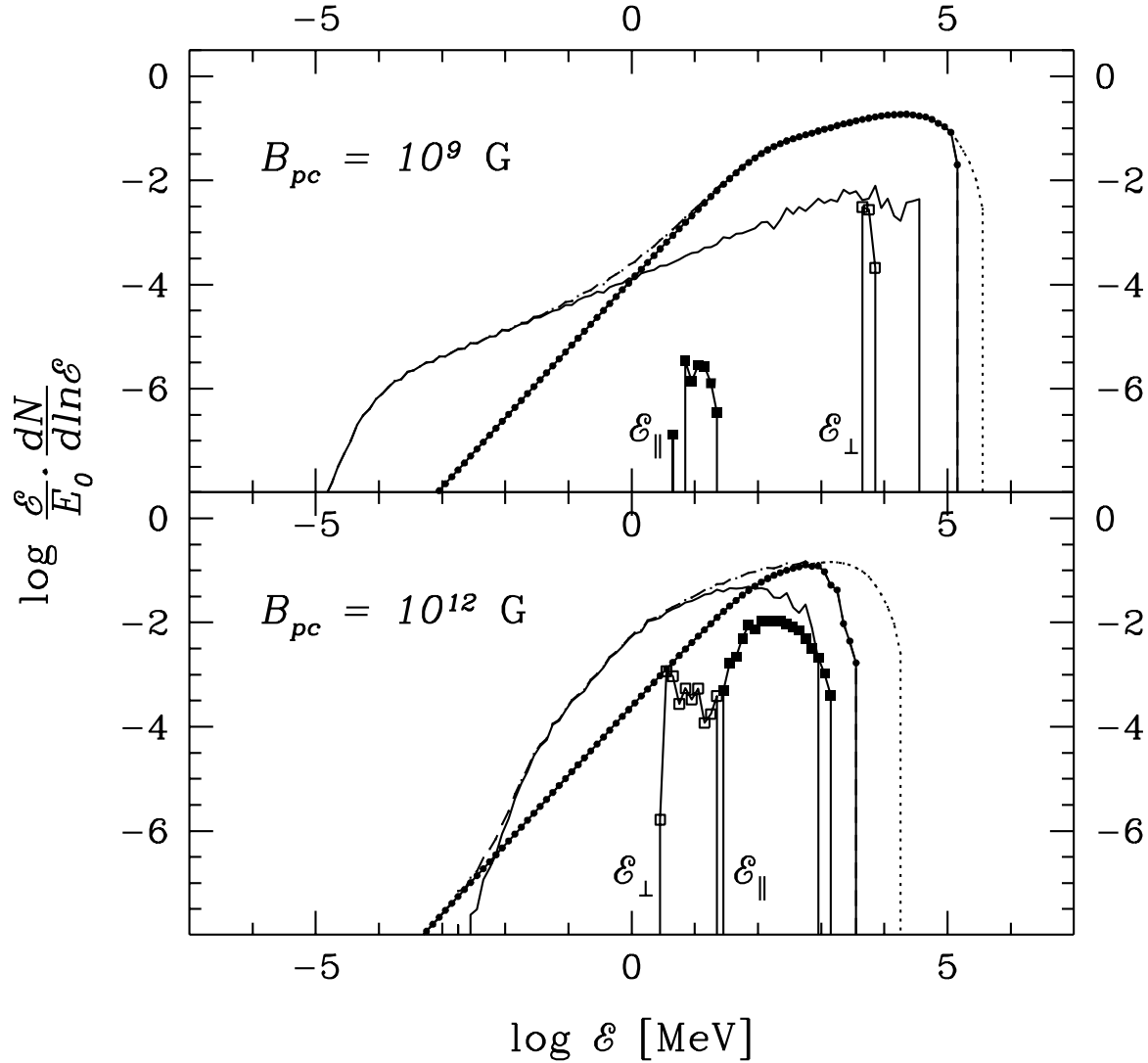


Figure 1. The radiation energy spectrum per logarithmic energy bandwidth. The spectrum is normalized to the energy of the parent particle, E_0 . It consists of two components: curvature and synchrotron. Dotted line is the curvature spectrum before correction for the magnetic absorption effects. Solid line connecting filled dots, is the curvature spectrum with the magnetic absorption taken into account. Solid line without any symbols overlayed is the synchrotron component. Dot-dashed line indicates superposition of the two.

In addition to the electromagnetic spectra, we show the spectra of e^\pm pairs: the line connecting filled squares is for the energy parallel to local magnetic field lines (labeled with \mathcal{E}_\parallel); the line connecting open squares is the initial distribution of energy perpendicular to local magnetic lines (labeled with \mathcal{E}_\perp).

The upper panel is for $B_{pc} = 10^9$ G, and $E_0 = 1.08 \times 10^7$ MeV (see eq.14) which corresponds to $P = 3.1 \times 10^{-3}$ s (i.e. $L_{sd} = 10^{35}$ erg s $^{-1}$). The lower panel is for $B_{pc} = 10^{12}$ G, and $E_0 = 6.68 \times 10^6$ MeV which corresponds to $P = 5.6 \times 10^{-2}$ s (i.e. $L_{sd} = 10^{36}$ erg s $^{-1}$).

around 0.1 keV, i.e. in the soft range of X-rays. More importantly, the SR component dominates over the CR component in the entire energy range of X-rays. The lower panel of Fig.1 shows analogous results obtained for $B_{pc} = 10^{12}$ G. The created pairs belong now to two generations, and they are rich (~ 400 times more numerous than for 10^9 G). Therefore, the SR component is now energetically comparable to CR. There is no single, well defined turnover energy ϵ_{ct} anymore.

The spectrum of the source function Q_\pm is spread over two decades in energy, and in consequence the SR spectrum reveals a gradual turnover, which starts already at ~ 1 MeV, due to high values of γ_\parallel as well as strong local B (see eq.13).

Our approximate treatment of SR spectral shapes at low-energy limit requires a word of comment: As electrons go to the ground Landau level, the spectrum reveals its harmonic structure and the analytical formula that we used,

should be treated with caution. Comparison of Monte Carlo spectra (calculated by summing-up the rates of the quantum transitions), with analytical formulae was carried out by Harding & Preece (1987). They found that the analytical formula for the low-energy tail of SR with a cutoff at cyclotron frequency generally overestimates (but not dramatically) the actual level of photon spectrum. Therefore, our results for SR in the context of X-rays should be treated rather as upper limits, but this does not change our conclusions.

3 RELATIONS BETWEEN X-RAYS AND GAMMA-RAYS

We calculated combined spectra of CR and SR (as shown in Fig.1), emitted by a beam particle with initial energy E_0 , for two canonical values of B_{pc} : 10^9 G and 10^{12} G, and for a range of periods P in order to cover a full possible range of spin-down luminosities L_{sd} . Formula for the energy E_0 was adopted from Rudak & Dyks (1998) [RD98]. This energy is only a few times higher than threshold energy E_{min} required for magnetic pair creation in a dipolar magnetic field:

$$E_0 = 2.5 \times E_{min}, \quad (14)$$

$$\text{with } E_{min} = 1.2 \times 10^7 \left(\frac{B}{10^{12} \text{ G}} \right)^{-1/3} P^{1/3} \text{ MeV}, \quad (15)$$

but at the same time it must never exceed any of the following limits – E_{max} and E_w (the first restriction is due to curvature cooling, the second one is due to potential drop across the polar cap). The original motivation for this formula was to reproduce L_γ for the seven gamma-ray pulsars. For 10^9 G, $E_0 \approx 10^7$ MeV, while L_{sd} covers the range between 10^{34} erg s $^{-1}$ and 10^{37} erg s $^{-1}$. In practice, the values of E_0 do not change dramatically over the allowed ranges of L_{sd} : For 10^{12} G, E_0 starts with 3×10^6 MeV, increases to 9.8×10^6 MeV, and goes down to 4×10^6 MeV, for L_{sd} changing from 10^{31} erg s $^{-1}$ to 10^{39} erg s $^{-1}$.

What became clear already in the previous section is that the range of X-rays is never energetically important. Although for 10^9 G the spectrum of SR extends well into soft X-ray band and dominates there, its fractional contribution to the total radiation energy output is low. It varies between 0.003 (for $L_{sd} = 10^{34}$ erg s $^{-1}$) and 0.22 (for 10^{37} erg s $^{-1}$). For the case of 10^{12} G, the energy content of SR becomes significant for $L_{sd} > 10^{33}$ erg s $^{-1}$, but the spectrum of SR is now confined to gamma-rays, and it turns over at $\lesssim 1$ MeV. In either case, the bulk of particle energy converted into radiation is concentrated within gamma-rays.

Gamma-ray luminosity L_γ in RD98 was identified with the power of outflowing particles

$$L_{particles} = \eta E_\pm n_\pm \dot{N}_{GJ}, \quad (16)$$

where E_\pm (characteristic energy attained by a fraction of secondary particles, ηn_\pm , due to possible acceleration) was assumed to be of the order of E_0 , and \dot{N}_{GJ} was the Goldreich-Julian rate of outflow of beam particles. The parameter $\eta = 0.004$ was used to match the model with the joint *EGRET* and *COMPTEL* luminosity inferred for B1951+32 (see RD98 for details). Here we made more accurate calculations for L_γ , by replacing the particle energy E_0 with its radiation energy yield E_γ for photon energy

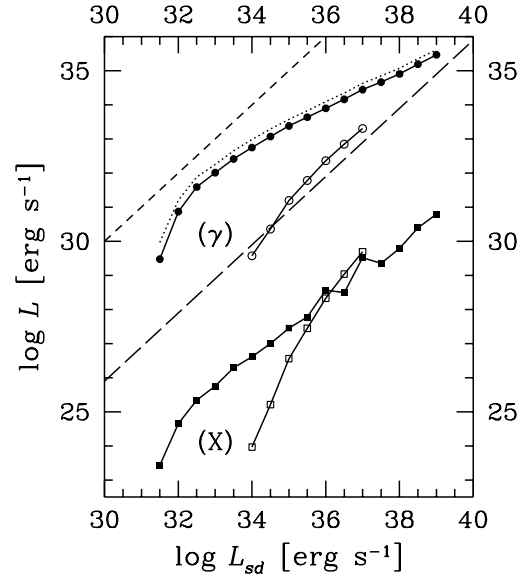


Figure 2. Evolution of high-energy, non-thermal luminosity across the spin-down luminosity space. The long upper curve connecting filled dots is the track of gamma-ray luminosity $L_\gamma (> 100$ keV), and the long lower curve connecting filled squares is the track of X-ray luminosity L_X (0.1 – 10 keV), both calculated according to eq.17, for a pulsar with $B_{pc} = 10^{12}$ G. [The dotted line is the track of $L_{particles}$ (eq.16), which in RD98 was identified with L_γ .]

The short upper curve with open circles is for gamma-ray luminosity $L_\gamma (> 100$ keV), and the short lower curve with open squares is for X-ray luminosity L_X (0.1 – 10 keV), calculated according to eq.17, for $B_{pc} = 10^9$ G. The short-dashed line marks $L = L_{sd}$. The long-dashed line, marking the empirical relation of Becker & Trümper (1997) rewritten for $\Omega_X = 1$ sr, has been added for reference. The fluctuations of L_X (0.1 – 10 keV) (for 10^{12} G only) between 10^{36} erg s $^{-1}$ and 10^{37} erg s $^{-1}$ in L_{sd} , are of numerical origin: in this range of L_{sd} the low-energy tail of the synchrotron component crosses the curvature component just around 10 keV, and any fluctuations due to Monte Carlo treatment of cutting off synchrotron spectra influence the level of the total spectrum.

$\epsilon \geq 100$ keV. Similarly, we calculate expected X-ray luminosity L_X within (0.1 keV – 10 keV). Accordingly, we take

$$L_\gamma = L_{particles} \times \frac{E_\gamma}{E_0}, \text{ and } L_X = L_{particles} \times \frac{E_X}{E_0}, \quad (17)$$

where $\frac{E_\gamma}{E_0}$ and $\frac{E_X}{E_0}$ are fractional radiation energy yields per particle, calculated by integrating the differential (per logarithmic energy bandwidth) spectra [which are simply

$$\frac{1}{E_0} \epsilon \frac{dN_\nu}{d \ln \epsilon} \quad (18)$$

– see Fig.1 for two examples], over the range $\epsilon \geq 100$ keV and $0.1 \text{ keV} \leq \epsilon \leq 10 \text{ keV}$, respectively.

Extremely low values of relative energy output in X-ray photons and gamma-ray photons per particle imply equally low values of L_X/L_γ (between 10^{-6} and 10^{-4}). Fig.2 presents L_γ and L_X calculated according to eqs.17, 18, and 16 as a function of L_{sd} . It shows unambiguously, that some pulsars from the list of X-ray and gamma-ray source do not

fit the picture: The Crab pulsar, for which the observed ratio of L_X/L_γ is about 0.47, remains certainly a challenge. Also among millisecond pulsars, there is a ‘Crab-like’ example, which does not fit the model. B1821-24 observed with *ASCA* (Saito et al. 1997) reveals clear, double-peaked pulsations resembling those of the Crab. Apart of the disagreement between the observed spectral slope (~ 1.9) and the predicted one (~ 1.5), the predicted ratio of $L_X/L_\gamma \sim 2 \times 10^{-4}$ (we took L_X for 1sr) would make L_γ to exceed L_{sd} . Or, alternatively, using the upper limit for the gamma-ray luminosity, $L_\gamma < 0.028 L_{sd}$ (Nel et al. 1996), the “observed” ratio L_X/L_γ is $> 2.5 \times 10^{-3}$, in disagreement with predictions.

However, among pulsars there are also strong sources of steady X-ray emission, with no trace of pulsations. B1706-44, a strong gamma-ray pulsar detected with *EGRET*, with $L_\gamma = 2.5 \times 10^{34}$ erg s $^{-1}$ (Thompson et al. 1996) shows no pulsations in X-rays. Its unpulsed, non-thermal X-ray emission has the luminosity $L_X = 1.3 \times 10^{33}$ erg s $^{-1}$ (Becker et al. 1993). Apparently, pulsed X-rays of B1706-44, which we predict to reach the luminosity of $\sim 3 \times 10^{29}$ erg s $^{-1}$, are dwarfed by nearby nebular steady emission.

4 CONCLUSIONS

Recent results from *ROSAT* and *ASCA* suggest that the X-ray spectra of pulsars may be a superposition of thermal and non-thermal components (see e.g. Zavlin & Pavlov 1997 for discussion). The existence of these two components is in general expected in both classes of rival models (polar-cap and outer-gap models; e.g. Arons 1981 and Cheng, Ho & Ruderman 1986, respectively) and the thermal component results from polar cap heating by inflowing particles. However, clear empirical relations between thermal and non-thermal components are yet to be determined. The latest review on the status of pulsar X-ray properties by Becker & Trümper (1997) favours pure non-thermal spectral models (with four exceptions of additional thermal components due to initial cooling of the star itself).

Within the framework of polar-cap models with magnetospheric activity induced by curvature radiation of beam particles we have calculated broad-band photon spectra of non-thermal origin, for both classical and millisecond pulsars. This non-thermal emission is a superposition of curvature and synchrotron radiation. It is expected to be pulsed, like its high-energy extension - the gamma-ray emission. Our objective was to estimate spectral properties and the level of this emission in the energy domain of X-rays.

Our calculations show, that for beam particles with monoenergetic source function, the properties of photon spectra in the combined energy range for *ROSAT* and *ASCA* (0.1 - 10 keV) depend primarily on the magnetic field strength at the polar cap. Millisecond pulsars, with dipolar magnetic fields of the order of 10^9 G, have X-ray spectra dominated by synchrotron emission. On the other hand, pulsars with B of the order of 10^{12} G have X-ray spectra almost exclusively due to low-energy tail of curvature emission. However, the spectrum of the curvature component breaks already at 150 MeV regardless the pulsar parameters, and neither its slope nor level in the X-ray domain is compatible with phase-averaged spectra of pulsed X-ray emission inferred from observations.

Detailed properties of the broad-band spectrum, depend upon the location(s) of cyclotron turnover energy $\epsilon_{ct} = \hbar \frac{eB}{m_e c} / \sin \psi$ of the synchrotron emission. Unlike in outer-gap models, the available range of pitch angles ψ is rather narrow and confined to low values ($\sin \psi < 0.01/\sqrt{P}$). We find that for classical pulsars (10^{12} G) the upper limit for turnover energy ϵ_{ct} occurs already at ~ 1 MeV. Below this energy, the level of synchrotron spectrum gradually decreases, and around ~ 10 keV the curvature component takes over. Unless the spectrum of primary beam particles is very steep ($N_b \propto \gamma_b^{-4}$) and extends down to Lorentz factor $\gamma_b \approx 10^5$, the X-ray spectrum below ~ 10 keV is a power-law with photon index $\alpha_{ph} = 2/3$. Therefore, the model is not able to explain the non-thermal X-ray spectra with $\alpha_{ph} \simeq 1.5 \div 2$ inferred from observations (Becker & Trümper 1997).

The expected luminosity L_X of pulsed component is a negligible fraction of gamma-ray luminosity L_γ , and for $L_{sd} \geq 10^{33}$ erg s $^{-1}$ an approximate relation

$$\log L_X \approx -1.5 + 0.83 \log L_{sd} \quad (19)$$

follows from Fig.2. The situation is qualitatively different for millisecond pulsars. The X-ray spectra are dominated now by synchrotron components, with a photon index $\alpha_{ph} \simeq 3/2$, which extends down to $\epsilon_{ct} \sim 100$ eV before breaking sharply into $\alpha_{ph} \simeq -1$. The expected L_X is still low with respect to L_γ , though not as low as for classical pulsars. For $L_{sd} \geq 10^{34}$ erg s $^{-1}$ we find

$$\log L_X \approx -40.3 + 1.90 \log L_{sd}. \quad (20)$$

We conclude that spectral properties and fluxes of pulsed non-thermal X-ray emission of some objects, like the Crab or the millisecond pulsar B1821-24, pose a real challenge to the subclass of polar-cap models based on curvature and synchrotron radiation alone.

ACKNOWLEDGEMENTS

This work has been financed by the KBN grant 2P03D-00911. BR acknowledges discussions with K.S. Cheng, J. Gil, and W. Kluźniak. We thank the anonymous referee for useful suggestions which helped to clarify the paper.

REFERENCES

- Arons J., 1981, ApJ, 248, 1099
- Becker W., 1995, Ph.D. Thesis (LMU Munich)
- Becker W., Brazier K.T.S., Trümper J., 1993, A&A, 273, 421
- Becker W., Trümper J., 1997, A&A, 326, 682
- Cheng K.S., Gil J., Zhang L., 1998, ApJ, 493, L35
- Cheng K.S., Ho C., Ruderman M.A., 1986, ApJ, 300, 500
- Daugherty J.K., Harding A.K., 1982, ApJ, 252, 337
- Daugherty J.K., Harding A.K., 1996, ApJ, 458, 278
- Dermer C.D., Sturmer S.J., 1994, ApJ, 420, L75
- Harding A.K., Preece, R.T., 1987, ApJ, 319, 939
- Manning R.A., Willmore A.P., 1994, MNRAS, 266, 635
- Nel H.I. et al., 1996, ApJ, 465, 898
- O’Dell S.L., Sartori L., 1970, ApJ, 161, L63
- Rudak B., Dyks J., 1998, MNRAS, 295, 337 [RD98]
- Saito Y., 1998 in Shibata S., Sato M., eds. Proc. Neutron Stars and Pulsars. Universal Academy Press, Tokyo, in press

- Saito Y., Kawai N., Kamae T., Shibata S., Dotani T., Kulkarni S.R., 1997, ApJ, 477, L37
- Thompson D.J. et al. 1996, ApJ, 465, 385
- Thompson D.J., Harding A.K.H., Hermsen W., Ulmer M.P., 1997, in Dermer C.D., Strickman M.S., Kurfess, J.D., eds, AIP Conf. Proc. 410, 4th Compton Symposium. AIP, New York, in press
- Wang F.Y.-H., Halpern J.P., 1997, ApJ, 482, L159
- Wang F.Y.-H., Ruderman M., Halpern J.P., Zhu T., 1997, preprint (astro-ph/9711283)
- Zhang L., Cheng K.S., 1997, ApJ, 487, 370
- Zhavlin V.E., Pavlov G.G., 1998, A&A, 329, 583